

Vibrational, Optical, Molecular Docking, Potential Energy Surface and Thermodynamic Properties of N, N-Dimethylnicotinamide

G. John James^{1*}, Senthilkumar Chandran², M. Arivazhagan¹

¹Department of Physics, Government Arts College, Tiruchirappalli, Tamilnadu-620022

²Department of Physics, Government Arts College, Hosur, Tamilnadu- 635109

Abstract:- The experimental and computational analysis of the geometrical structure and vibrational wavenumber of N, N-dimethylnicotinamide is determined. The FTIR and FT-Raman analyses were carried out and vibrational frequencies are compared with the quantum chemical computational methods. First-order hyperpolarizability and dipole moment values are calculated. The UV-Vis properties were registered by UV-Vis-NIR analysis. The total energy of N, N-dimethylnicotinamide is -495.5720 Hartrees. Different thermodynamic properties are calculated and the results are compared with HF and B3LYP methods. The auto docking is also carried out for N, N-dimethylnicotinamide molecule.

Keywords:- Molecular Structure; Vibrational Analysis; Optical Properties; Molecular Docking.

I. INTRODUCTION

In recent years, peoples are severely affecting by cancer and skin diseases. Several reports show that nicotinamide may have anti-inflammatory action against cancer and skin diseases. It is also used in cosmetic, stroke, diabetes mellitus, psoriasis vulgaris, and some other diseases. Nicotinamide structure contains a pyridine ring through the amide group. N, N-dimethylnicotinamide (NNDMN) has several biological and pharmaceutical activity [1, 2]. Still, now there is no report on quantum chemical calculations of NNDMN. The quantum chemical calculation is an efficient tool to study the vibrational analysis of biological and natural products [3-5]. Recent years, quantum chemical calculation approaches are used to find out the molecular structural, vibrational, optical and electrochemical features of molecular structures. Therefore, the appropriate quantum chemical technique allows the researchers to calculate the molecular physical features frugally and to clarify some research phenomena perceptively. Consequently, it is essential to emphasize that the theoretical methods realized form DFT/B3LYP computation level are more real and consistent as compared to those concluded from the other approaches [6-8]. Hence, a systematic investigation is carried out on N, N-dimethylnicotinamide molecule using quantum chemical calculations employing DFT and HF approaches with 6-311+G(d,p) basis set. This paper reports, the molecular structure, atomic charges, HOMO-LUMO, first

hyperpolarizability, UV-Vis, thermodynamic, potential energy surface and molecular docking analyses of NNDMN molecule.

II. EXPERIMENTAL PROCEDURE

2.1 Experimental analysis

The N, N-dimethylnicotinamide was obtained from Sigma-Aldrich chemical company. The FTIR spectrum was a registrar from 4000 to 500 cm^{-1} using BRUKER spectrometer fitted through MCT detector through ATR mode by the resolution of 1 cm^{-1} . The FT-Raman was registered from 4000 to 50 cm^{-1} by BRUKER RFS 27 standard alone unit by the resolution of 4 cm^{-1} . Nd: YAG laser (1064 nm) with InGaAs and proprietary high-sensitivity Ge detector was used for the experiment. Liquid nitrogen was used for cooling purpose. The UV-Vis was registered by Perkin Elmer LAMBDA 950 in the region from 200 to 800 nm with slit width 2 nm. PMT (UV-VIS) and Peltier cooled PbS (NIR) detectors were used for the experiment. All the experiments were carried out using a liquid sample.

2.2. Computational methods

The quantum computations were executed at Hartree-Fock (HF) and density functional theory (DFT) by GAUSSIAN 09W [9]. The optimized geometric parametric quantity was applied for the atomic charges, HOMO-LUMO, first hyperpolarizability, UV-Vis, vibrational, molecular electrostatic potential energy (MEP), potential energy surface (PES) and thermodynamic calculations. The total energy distribution is executed using MOLVIB program (version V7.0-G77). Using the GAUSSVIEW 5.0 software, optimized structure, HOMO-LUMO, electrostatic potential energy and potential energy surface were visualized [10].

III. RESULTS AND DISCUSSION

3.1. Explanation of NNDMN structure

The molecular structure of NNDMN is displayed in Fig. 1. NNDMN contains owns fifty-seven normal modes of vibrations and twenty-one atoms. These modes are dynamic in infrared and Raman. It has a C_1 point group symmetry. From Table S1 (supplementary information file (SIF)), the accuracy of bond angles and bond lengths of the B3LYP/6-311+G(d,p) method is somewhat higher than HF/6-311+G(d,p) levels. However, the B3LYP method values are

in good accord with the HF level. For NNDMN, the sturdy bonds are formed among C3-C8 (1.4978 Å) and C-H methyl group (C11-H13, C11-H14, C11-H15, C12-H16, C12-H17, and C12-H18) (bonds were ~1.08 Å), that possess tiny bond length value associated to others. The bond angle of C2-N1-C6, N1-C2-C3, N1-C2-H7, C11-N10-C12, and N10-C11-H13 are 118.9222/118.0490, 122.7560/123.1958, 115.9516/115.7350, 115.0998/115.3582 and 109.0248/109.1984 in HF/B3LYP, respectively. The dihedral angle values of C6-N1-C2-C3, H7-C2-C3-C4, C3-C8-N10-C12 and O9-C8-N10-C11 are -0.1446/-0.0730, 177.5399/177.1510, 171.6890/172.8871 and 160.5591/164.8762 in HF/B3LYP, respectively. In the present manuscript, a few essential geometrical parameters are deliberated, additional geometrical parameters were specified in Table S1.

3.2 FTIR and FT-Raman analyses

The vibrational study of NNDMN is executed with the support of normal coordinate exploration. The vibrational assignments are recorded in Table S2. The FTIR and FT-Raman spectra of NNDMN are displayed in Figs. 2 and 3, severally.

C-H and CH₃ vibrations

The range from 3100 to 3000 cm⁻¹ are contributed to the C-H stretching wavenumbers [11, 12]. These vibrational wavenumbers are noted at 3196, 3071 cm⁻¹ in Raman whereas computed at 3198/3196, 3098/3091 and 3075/3069 cm⁻¹ in HF/B3LYP, respectively. The C-H in-plane bending vibrations are calculated at 1375/1368, 1292/1288 cm⁻¹ in HF/B3LYP. Bands found at 730, 715, 650 cm⁻¹ in IR and at 750/641, 733/725 and 667/659 in cm⁻¹ in HF/B3LYP are due to the C-H out-of-plane bending modes. The CH₃ group has nine fundamental vibrations. The symmetric and asymmetric stretching modes (CH₃) are obtained at 2905-2940 and 2925-3000 cm⁻¹, respectively [13, 14]. The CH₃ symmetric stretching modes are noted at 3040 cm⁻¹ in IR whereas the equivalent band is computed (HF/B3LYP) at 3050/3045 cm⁻¹. The CH₃ asymmetry in-plane stretch vibration is noted at 2980 cm⁻¹ in Raman and computed (HF/B3LYP) at 2968/2963 cm⁻¹ [15]. The CH₃ out-of-plane stretching modes are obtained at 2941 cm⁻¹ in IR and 2940, 2815 cm⁻¹ in FT-Raman. The comparable wavenumbers are calculated at 2929/2925 and 2824/21818 cm⁻¹ in HF/B3LYP, respectively. The CH₃ out-of-plane bending wavenumbers are perceived at 1201, 1192 cm⁻¹ (IR) and 1191 cm⁻¹ (Raman) and corresponding bands are computed (HF/B3LYP) at 1218/1213 cm⁻¹. The CH₃ in-plane rocking modes are assigned at 1060, 1040 cm⁻¹ in FTIR and 1036 cm⁻¹ in Raman whereas computed at 1073/1068 and 1054 in HF/B3LYP, respectively. CH₃ in-plane rocking mode is noted at 1122 cm⁻¹ in FTIR and comparable band computed at 1133/1130 in HF/B3LYP.

C-C, C-O, and C-N vibrations

The bands obtained from 1400 to 1650 cm⁻¹ are contributed to the C-C stretching vibrations of benzene derivatives [16, 17]. The C-C stretching modes are obtained at 1621 in IR, 1596 cm⁻¹ in Raman and corresponding bands are calculated at 1629/1623 and 1596/1592 in HF/B3LYP. The C-C ring in-plane bending modes are noted at 1221 cm⁻¹ while calculated (HF/B3LYP) at 1238/1231 cm⁻¹. The C=O stretching modes of vibration is calculated at 1781/1693 cm⁻¹ in HF/B3LYP. In heteroaromatic compounds, the region from 1400 to 1200 cm⁻¹ is contributed to the C-N stretching vibration. The C-N stretching modes are noted at 1502, 1459 cm⁻¹ in IR, 1516 cm⁻¹ in FT-Raman whereas calculated (HF/B3LYP) at 1510/1504, 1479/1471 cm⁻¹. Apart from these vibrations C-O, C-N bending vibrations and deformations are also given in Table S2.

3.3 Highest occupied molecular orbital-(HOMO) lowest unoccupied molecular orbital (LUMO) analysis

HOMO-LUMO values of materials are significant quantum mechanical descriptors and really helpful to elucidate its reactivity. It acts as an important character in optical and charges transport properties. The LUMO describes the ability to accept electron (which can be thought-about the inner orbital bearing a free position to receive electrons) and HOMO signifies the power to give electron (which can be thought-about the outer orbital having electrons). The calculated HOMO and LUMO values are -0.36788 a.u and 0.05855 a.u, severally. The band gap energy is 0.30933 a.u. It provides the charge transfer inside the molecule (Fig. 4).

3.4 First order hyperpolarizability

In recent years, DFT is a powerful method to find out the nonlinear optical properties (NLO) of the materials. It provides the data concerning the connection among the molecular structure and NLO features. To recognize nonlinear properties of the NNDMN, computation of the dipole moment (μ) and first hyperpolarizability (β) were performed by the DFT/B3LYP method. **The dipole moment can be given as:**

$$\mu_{total} = \mu_0 + \alpha_{ij}E_j + \beta_{ijk}E_{ijk}E_jE_k + \dots \quad (1)$$

where, α is the linear polarizability, $\mu_{(0)}$ is the dipole moment and β_{ijk} is the hyperpolarizability. The dipole moment (μ) can be estimated by the expression [18,19]:

$$\mu = (\mu_x^2 + \mu_y^2 + \mu_z^2)^{\frac{1}{2}} \quad (2)$$

where, μ_x , μ_y , and μ_z are dipole moments along x, y and z directions. First order hyper-polarizability tensor could be represented by $3 \times 3 \times 3$ matrices. Using Kleinmann symmetry [20]. The twenty-seven components of the three-dimensional matrix can be minimized to ten components. Using the density functional theory calculations, we obtain ten components (β_{xxx} , β_{xyx} , β_{xyy} , β_{yyy} , β_{xxz} , β_{xyz} , β_{yyz} , β_{xzz} , β_{yzz} and β_{zzz}). The value of the total first-order hyperpolarizability (β_{total}) tensor may be determined by the subsequent expression [7, 21]:

$$\beta_{total} = (\beta_x^2 + \beta_y^2 + \beta_z^2)^{\frac{1}{2}} \quad (3)$$

where

$$\beta_x = \beta_{xxx} + \beta_{xyx} + \beta_{xxz}, \beta_y = \beta_{yyy} + \beta_{yyz} + \beta_{xyy}, \beta_z = \beta_{zzz} + \beta_{yzz} + \beta_{xzz}$$

Theoretically measured first hyperpolarizability and dipole moment for NNDMN are 0.905696×10^{-30} esu and 3.3075 Debye, whereas in the case of urea molecule found to be 1.3732 Debye and 0.3728×10^{-30} esu, severally. The NLO properties of materials depend upon the hyperpolarizability. NNDMN has good hyperpolarizability value. The hyperpolarizability of the NNDMN is higher than the urea molecule. The hyperpolarizability value of NNDMN is compared with other organic molecules. Hence, the higher first hyperpolarizability and dipole moment values recommended that the NNDMN molecule is suitable for non-linear optical characteristics. The first order hyperpolarizability of NNDMN molecule is compared with some organic molecules and it is given in Table 1 [6, 8, 188, 22, 23].

3.5 Mulliken's population analysis

The charge distribution of NNDMN is depicted in Fig. 5. The C3(1.0884) atom has a more positive charge and C4 (-0.0890) own more negative in NNDMN molecule (Table 2). The O9, N1 atoms have the negative charge whereas all H atom has a positive charge. In the case of carbon atoms both positive (C3 and C5) and negative charges (C2, C4, C6, C8, C11 and C12) are obtained.

3.6 UV-Visible study

The UV-Vis of NNDMN recorded and computed in the water phase is shown in Fig. 6. Theoretical results are correlated with recorded experimental wavelength and listed in Table 3. The electronic transition at 236 nm predicted by experimental whereas in TD-DFT it is observed at 256 nm by an oscillator strength of 0.0039 (Table 3). The absorption is due to the $\pi \rightarrow \pi^*$ transition. The absorption found out in the UV-Vis spectrum may be owing to the electronic transition takes place from HOMO-LUMO, HOMO+1 – LUMO, HOMO+2 – LUMO and HOMO – LUMO+1. The other computed peaks noted at 360 nm, 378 nm by the oscillator strength values of 0.0048 and 0.0043 and transitions are HOMO – LUMO, HOMO+1 – LUMO, HOMO+2 – LUMO and HOMO – LUMO+1.

3.7 Molecular electrostatic potential (MEP)

MEP give various spacious intuitive regarding the dissemination of electrostatic charges on the optimized basis state structure of NNDMN molecule. The charge distribution of the molecule is represented by the color coding. For example, an extreme negative area is desired position as the electrophilic attack that is shown as red color surface whereas the utmost positive area that is desired position for nucleophilic attack specified as blue color on the molecular electrostatic potential surface. The light blue color displays somewhat electron poor area and yellow spectacles the somewhat electron-rich area. The negative electrostatic potential position area is confined in the O atom whereas H and N (C-attached) atoms own positive electrostatic potential position (Fig. 7(a)). The contour plot of the NNDMN molecule is displayed in Fig. 7(b). It provides the various negative and positive position of the NNDMN in accordance with the entire electron density surface.

3.8 Potential energy surface

To outline the preferential location of N, N-dimethylnicotinamide with regard to methyl group an initial exploration of the low-energy structure was executed by an equivalent basis set as a operate of (C4–C3–C8–N10) within the interval of 36° within the value 0° and 360° . The total energy of N, N-dimethylnicotinamide is -495.5720 Hartrees. Molecular energy curves with relevance rotations regarding the chosen dihedral angles are conferred in Fig. 8. Within the rotation of (C4–C3–C8–N10), the actively most affirmative structure is that the one at 180° with the value of -495.5810 Hartrees. These smallest energies indicate that CH₃ is creating the intermolecular hydrogen bonding at this position. For this methyl rotation three most energies are found at 0° , 180° and 360° that clearly suggests that this methyl has no likelihood of making the intermolecular bonding. So the foremost disapproving structure is found at 360° . Hence, PES scan computations predict the being of three completely diverse conformations of N, N-dimethylnicotinamide.

3.9 Thermodynamic properties

The computed thermodynamic properties are specified in Table 4. The ZPVE, rotational constants and thermal energy of HF and B3LYP are 115.5778, 107.8587 kcal mol⁻¹, 2.5004, 2.4395 GHz and 121.6910, 114.3630 kcal mol⁻¹, respectively. These show that the B3LYP method has low values as compared with the HF method. The calculated entropy and capacity constant volume are 97.6750, 100.5130 cal mol⁻¹ kelvin, 35.0530, 37.7010 cal mol⁻¹ k⁻¹ for HF and B3LYP, respectively. The entropy and molar capacity constant volume of HF method is lower than the DFT/B3LYP method.

3.10 Molecular docking

Molecular docking is employed to determine the intermolecular compound configuration amid two or a lot of molecules. The remarkable event is protein-ligand contact, owing to its practical application in medicine and drug design. There are a number of potential reciprocal conformations during which binding may happen. These are normally known as binding modes [24]. The crystal structure of pseudomonas aeruginosa LpxC compound was received from the protein data bank (PDB ID: 5N8C). The ligand binding active site of NNDMN is shown in Fig. 9. There are several numbers of possible docking pose, but hydrogen bonds were observed between the amino acid residue SER252 in the title molecule. These ensue recommend that the NNDMN exhibits repressing activity against LpxC complex.

IV. CONCLUSION

The optimized structure of NNDMN executed by HF and B3LYP with 6-311+G(d,p) basis set. The accuracy of bond angles and lengths of the B3LYP are slightly higher than the HF approach. The experimental vibrational wavenumber of NNDMN slightly deviated from the calculated wavenumbers. The band gap of title material is 0.30933 a.u. The first hyperpolarizability of NNDMN is 0.905696×10^{-30} esu. The atomic charges show that the C3(1.0884) atom has a more positive charge and C4(-0.0890) own more negative charge in NNDMN molecule. The electronic transition is predicted at 256 nm in TD-DFT whereas in experimental it is observed at 236 nm. MEP shows that O atom has negative electrostatic potential position area. PES scan computations predict the being of three completely diverse conformations of NNDMN. It is observed that the entropy and molar capacity constant is higher for B3LYP approach compared with the HF method. The NNDMN exhibits inhibitory activity against LpxC complex.

REFERENCES

- [1]. N. Otte, C. Borelli, H. C. Korting, Nicotinamide – biologic actions of an emerging cosmetic ingredient, *Int J Cosmet Sci*, 27 (2005) 255–261
- [2]. Ana R.R.P. Almeida, Juliana A.S.A. Oliveira, Manuel J.S. Monte, Thermodynamic study of nicotinamide, N-methylnicotinamide, and N,N-dimethylnicotinamide: Vapour pressures, phase diagrams, and hydrogen bonds, *J. Chem. Thermodynamics* 82 (2015) 108–115
- [3]. Q.Wang J.Xue, Y.Wang, S.Jin, Q.Zhang, Y.Du, Investigation into tautomeric polymorphism of 2-thiobarbituric acid using experimental vibrational spectroscopy combined with DFT theoretical simulation, *Spectrochim Acta Part A* 204 (2018) 99–104
- [4]. C.S. Nair Lakshmi, S. Balachandran, D. D. Arul, A. A. Ronaldo, J.I. Hubert, DFT analysis on spectral and NLO properties of (2E)-3-[4-(dimethylamino) phenyl]-1-(naphthalen-2-yl) prop-2-en-1-one; a d- π -A chalcone derivative and its docking studies as a potent hepatoprotective agent, *Chemical Data Collections* 20 (2019) 100205
- [5]. K. Sarojinidevi, P. Subramani, M.Jeeva, N. Sundaraganesan, M. SusaiBoobalan, G. V.Prabhu, Synthesis, molecular structure, quantum chemical analysis, spectroscopic and molecular docking studies of N- (Morpholinomethyl) succinimide using DFT method, *J. Mol. Struct.* 1175 (2019) 609-623
- [6]. S. Chinnasami, M. Manikandan, S.Chandran, R.Paulraj, P. Ramasamy, Growth, Hirshfeld surfaces, spectral, quantum chemical calculations, photoconductivity and chemical etching analyses of nonlinear optical p-toluidine p-toluenesulfonate single crystal, *Spectrochim Acta Part A* 206 (2019) 340–349
- [7]. D. Pegu, J.Deb, S.K.Saha, M.K.Paul, U. Sarkar, Molecular structure, chemical reactivity, nonlinear optical activity and vibrational spectroscopic studies on 6-(4-n-heptyloxybenzyloxy)-2-hydroxybenzylidene)amino)-2H-chromen-2-one: A combined density functional theory and experimental approach, *J. Mol. Struct.* 1160 (2018) 167-176.
- [8]. S. Chinnasami, S.Chandran, R.Paulraj, P. Ramasamy, Structural, vibrational, Hirshfeld surfaces and optical studies of nonlinear optical organic imidazolium L-tartrate single crystal, *J. Mol. Struct.* 1179 (2019) 506-513
- [9]. M.J. Frisch, G.W. Trucks, H.B. Schlegel, G.E. Scuseria, M.A. Robb, J.R. Cheesman, V.G. Zakrzewski, J.A. Montgomery, Jr., R.E. Stratmann, J.C. Burant, S. Dapprich, J.M. Millam, A.D. Daniels, K.N. Kudin, M.C. Strain, O. Farkas, J. Tomasi, V. Barone, M. Cossi, R. Cammi, B. Mennucci, C. Pomelli, C. Adamo, S. Clifford, J. Ochterski, G.A. Petersson, P.Y. Ayala, Q. Cui, K. Morokuma, N. Rega, P. Salvador, J.J. Dannenberg, D.K. Malich, A.D. Rabuck, K. Raghavachari, J.B. Foresman, J. Cioslowski, J.V. Ortiz, A.G. Baboul, B.B. Stetanov, G. Liu, A. Liashenko, P. Piskorz, I. Komaromi, R. Gomperts, R.L. Martin, D.J. Fox, T. Keith, M.A. Al-Laham, C.Y. Peng, A. Nanayakkara, M. Challacombe, P.M.W. Gill, B. Johnson, W. Chen, M.W. Wong, J.L. Andres, C. Gonzalez, M. Head-Gordon, E.S. Replogle, J.A. Pople, GAUSSIAN 09, Revision A 11.4, Gaussian, Inc, Pittsburgh PA, 2009.
- [10]. A. Frisch, A.B. Nielson, A.J. Holder, Gaussview User Manual, Gaussian Inc., Pittsburg, PA, 2000.
- [11]. S. Ramalingam, S. Periandy, S. Mohan, Vibrational spectroscopy (FTIR and FTRaman) investigation using ab initio (HF) and DFT (B3LYP and B3PW91) analysis on the structure of 2-aminopyridine, *Spectrochim. Acta A* 77 (2010) 73-81.

- [12]. V. Krishnakumar, N. Prabavathi, Analysis of vibrational spectra of 1-chloro-2,4-dinitrobenzene based on density functional theory calculations, *Spectrochim. Acta A* 72 (2009) 738-742.
- [13]. Clemy Monicka, C. James, FT-Raman and FTIR spectra, DFT investigation of the structure and vibrational assignment of mefenacet, *J. Mol. Struct.* 1095 (2015) 1-7.
- [14]. S. Jeyavijayan, J. Senthil Kumar, Structural, vibrational spectroscopic studies and quantum chemical calculations of 4-fluoro-3-methylphenol, *Der Chemica Sinica*, 7 (2016) 42-52
- [15]. M. Muniz-Miranda, Adsorption mechanism of 2-amino,5-nitropyrimidine on silver substrates, as detected by surface-enhanced Raman scattering, *Vibr. Spectr.* 29 (2002) 229-233.
- [16]. G. Socrates, *Infrared and Raman Characteristic Group Frequencies – Tables and Charts*, third ed., Wiley, Chichester, 2001.
- [17]. P.B. Nagabalasubramanian, S. Periandy, S. Mohan, M. Govindarajan, FTIR and FT Raman spectra, vibrational assignments, ab initio, DFT and normal coordinate analysis of α,α dichlorotoluene, *Spectrochim. Acta A* 73 (2009) 277-280.
- [18]. R. Thirumurugan, B. Babu, K. Anitha, J. Chandrasekaran, Synthesis, growth, characterization, and quantum chemical investigations of a promising organic nonlinear optical material: thiourea-glutaric acid, *J. Mol. Struct.* 1171(2017) 915-925.
- [19]. C.S. Abraham, J.C. Prasana, S. Muthu, Quantum mechanical, spectroscopic and docking studies of 2-Amino-3-bromo-5-nitropyridine by Density Functional Method, *Spectrochim Acta Part A* 181 (2017) 153–163.
- [20]. D.R. Kanis, M.A. Ratner, T.J. Marks, Design and construction of molecular assemblies with large second-order optical nonlinearities. Quantum chemical aspects, *Chem. Rev.* 94 (1994) 195–242.
- [21]. D.A. Kleinmann, Nonlinear Dielectric Polarization in Optical Media. *Phys. Rev.* 126 (1962) 1977–1979.
- [22]. V. Balachandran, G. Santhi, V. Karpagam, V.K. Rastogi, Structural features of the 2-amino-5-nitrobenzophenone by means of vibrational spectroscopy HF and DFT, first order hyperpolarizability, NBO, HOMO–LUMO and thermodynamic properties, *Spectrochim Acta Part A* 118 (2014) 835–846
- [23]. S. Sebastian, S. Sylvestre, N. Sundaraganesan, M. Amalanathan, S. Ayyapan, K. Oudayakumar, B. Karthikeyan, Vibrational spectra, molecular structure, natural bond orbital, first order hyperpolarizability, TD-DFT and thermodynamic analysis of 4-amino-3-hydroxy-1-naphthalenesulfonic acid by DFT approach, *Spectrochim Acta Part A* 107 (2013) 167–178.
- [24]. N.K. Sharma, K.K. Jha, Priyanka Molecular docking: an overview, *J. Adv. Sci. Res.*, 1 (2010) 67-72.

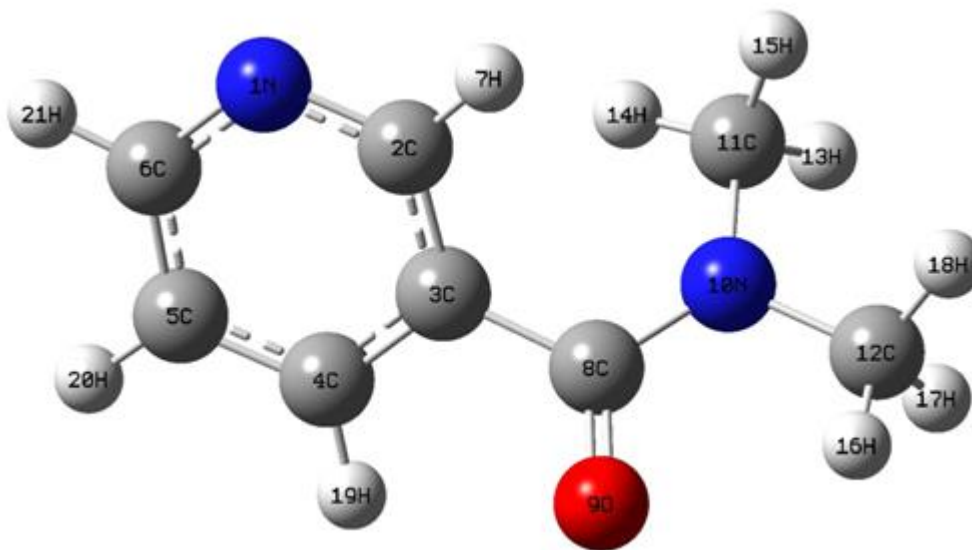


Fig. 1 Optimized molecular structure of N, N-Dimethylnicotinamide.

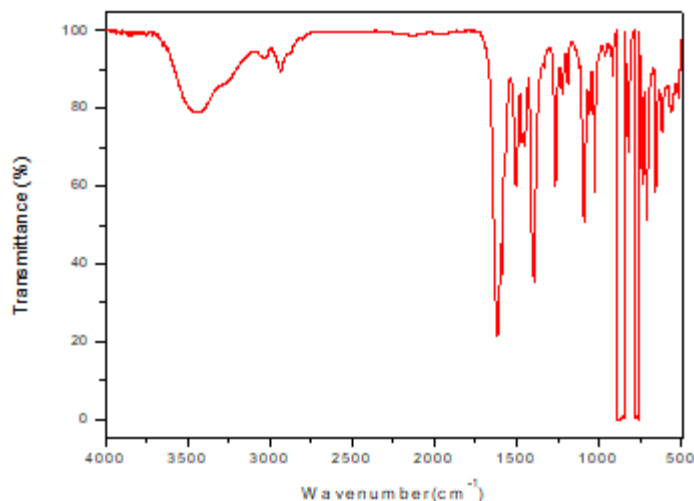


Fig. 2 FTIR spectrum of N, N-Dimethylnicotinamide.

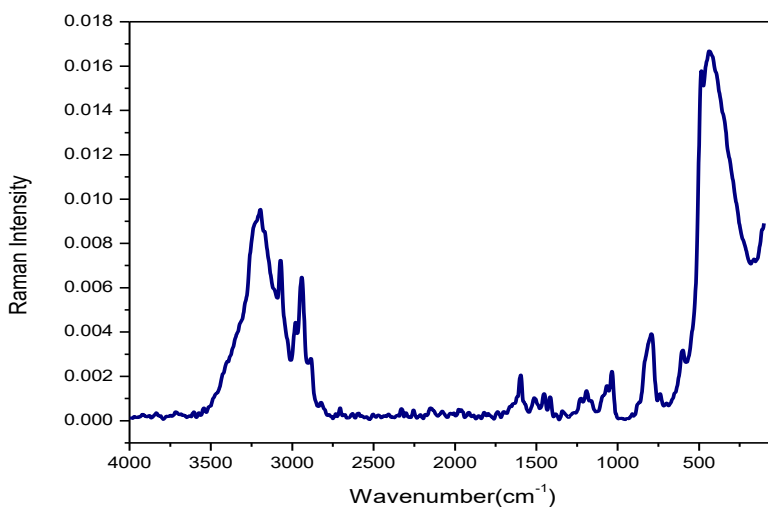


Fig. 3 FT-Raman spectrum of N, N-Dimethylnicotinamide.

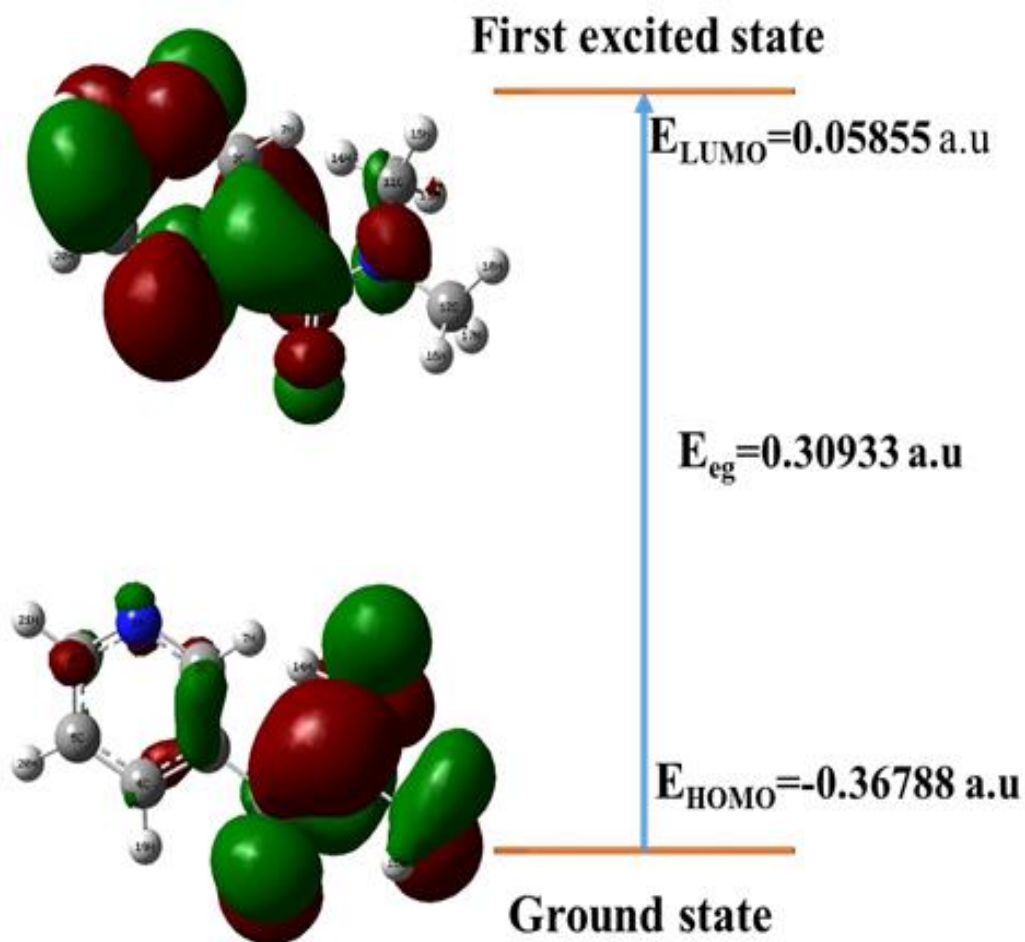
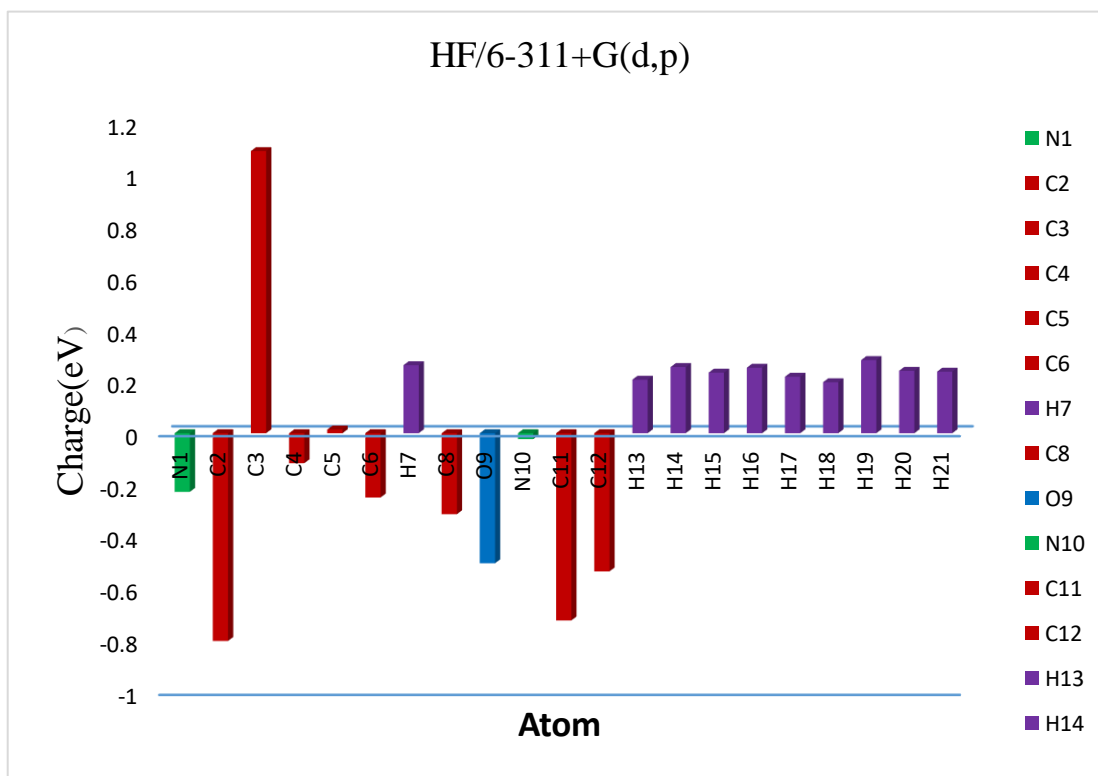


Fig. 4 Plots of HOMO, LUMO and the energy gap.



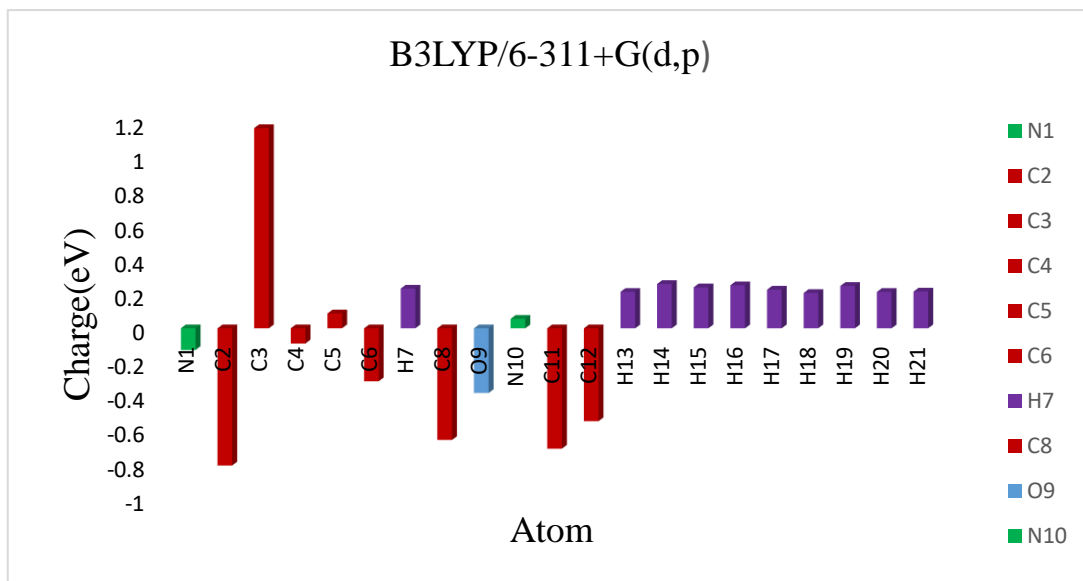


Fig. 5 Atomic charge plot of N, N-Dimethylnicotinamide.

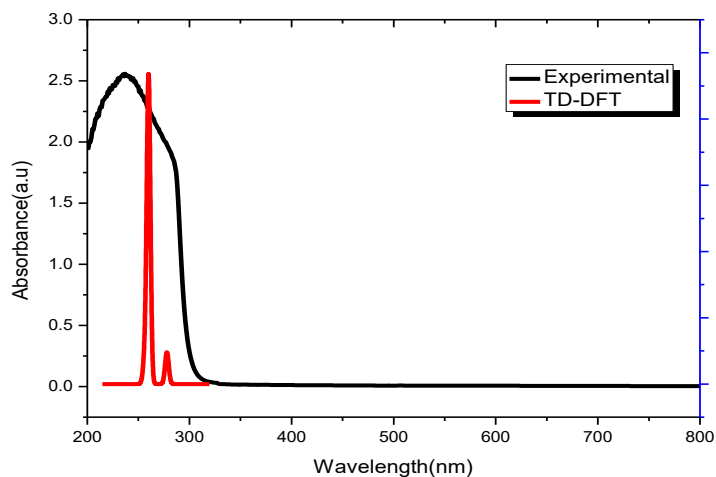


Fig. 6. UV-VIS Spectrum of N, N-Dimethylnicotinamide

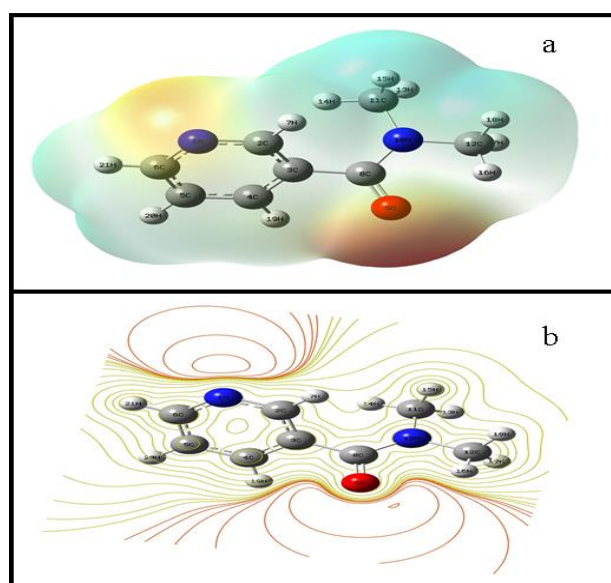


Fig. 7. (a) Molecular electrostatic potential and (b) Contour map of N, N-Dimethylnicotinamide

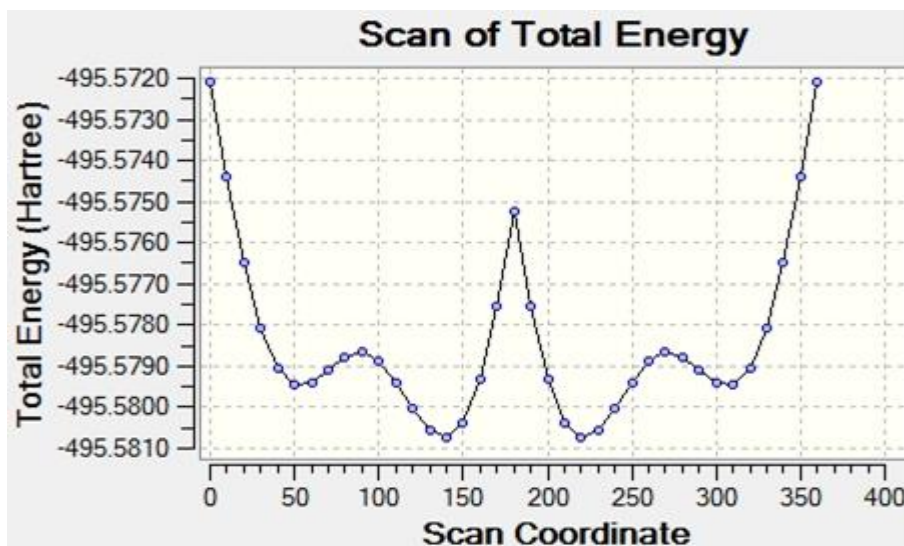


Fig. 8. SCAN conformers of N, N-Dimethylnicotinamide.

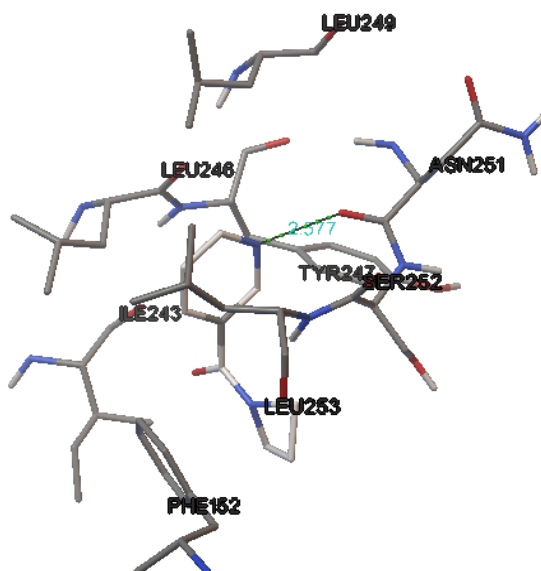


Fig. 9. Molecular docking of N, N-Dimethylnicotinamide.

Table 1 Comparison of first order hyperpolarizability value of N, N-dimethylnicotinamide with some organic molecules

Compound name	First order hyperpolarizability(β) $\times 10^{-30}$ esu	References
N,N-dimethylnicotinamide	0.905	Present work
Urea	0.372	Thirumurugan et al.[18]
2-amino-5-nitrobenzophenone	0.899	Balachandran et al. [22]
Imidazolium L-tartrate	1.257	Chinnasami et al [8]
4-amino-3-hydroxy-1-naphthalenesulfonic acid	2.941	Sebastian et al. [23]
p-toluidine p-toluenesulfonate	4.738	Chinnasami et al.[6]

Table 2 Atomic charge of N, N-Dimethylnicotinamide

Atom number	Atomic charges	
	HF	DFT/B3LYP
N1	-0.2262	-0.1265
C2	-0.8029	-0.8034
C3	1.0884	1.1683
C4	-0.1158	-0.0890
C5	0.0140	0.0867
C6	-0.2481	-0.3096
H7	0.2624	0.2315
C8	-0.3126	-0.6536
O9	-0.5017	-0.3781
N10	-0.0228	0.0553
C11	-0.7237	-0.7050
C12	-0.5333	-0.5432
H13	0.2064	0.2126
H14	0.2551	0.2584
H15	0.2336	0.2390
H16	0.2526	0.2508
H17	0.2178	0.2253
H18	0.1967	0.2062
H19	0.2820	0.2470
H20	0.2406	0.2125
H21	0.2374	0.2145

Table 3 The computed excitation energies, oscillator strength and electronic transition of N,N-Dimethylnicotinamide

Excited state	Singlet-A	Electronic absorption (eV)	Calculated Wavelength (nm)	Experimental Wavelength (nm)	Oscillator strength (f)	Transition
Excited state 1: 38 → 41	-0.1325	4.4605	278		0.0048	HOMO+2 - LUMO
	39 → 41	0.6212				HOMO+1 - LUMO
	40 → 41	-0.2755				HOMO - LUMO
Excited state 2: 39 → 41	0.2404	4.7683	260		0.0463	HOMO+1 - LUMO
	39 → 42	-0.1880				HOMO+1 - LUMO+1
	40 → 41	0.5975				HOMO - LUMO
	40 → 42	0.20174				HOMO - LUMO+1
Excited state 3: 37 → 41	-0.13309	4.8360	256	236	0.0039	HOMO+3 - LUMO
	38 → 41	-0.17929				HOMO+2 - LUMO
	39 → 41	0.11584				HOMO+1 - LUMO
	40 → 41	0.21127				HOMO - LUMO
	40 → 42	-0.22812				HOMO - LUMO+1

Table 4 Thermodynamic properties for N, N-Dimethylnicotinamide

Parameters	Values	
	HF	DFT/B3LYP
Zero-point vibrational energy (ZPVE) (kcal mol⁻¹)	115.5778	107.8587
Rotational Constants (GHz)		
A	2.5004	2.4395
B	0.7335	0.7197
C	0.6166	0.6093
Rotational Temperature (kelvin)		
D	0.1200	0.1170
E	0.0352	0.0345
F	0.0295	0.0292
Thermal Energy (kcal mol⁻¹)		
Total	121.6910	114.3630
Translational	0.8890	0.8890
Rotational	0.8890	0.8890
Vibrational	119.9140	112.5860
Entropy (cal mol⁻¹ kelvin)		
Total	97.6750	100.5130
Translational	40.9280	40.9280
Rotational	30.0310	30.0860
Vibrational	26.7160	29.4990
Molar capacity at constant volume (cal mol⁻¹ k⁻¹)		
Total	35.0530	37.7010
Translational	2.9810	2.9810
Rotational	2.9810	2.9810
Vibrational	29.0910	31.7390

Table S1 Optimized geometrical parameters of N,N-Dimethylnicotinamide

Bond length	Value (Å)		Bond angle	Value (°)		Dihedral angle	Value (°)	
	HF/ 6- 311+G(d,p)	B3LYP/ 6- 311+G(d,p)		HF/ 6- 311+G(d,p)	B3LYP/ 6- 311+G(d,p)		HF/ 6- 311+G(d,p)	B3LYP/ 6- 311+G(d,p)
N1-C2	1.3309	1.3499	C2-N1-C6	118.9222	118.0490	C6-N1-C2-C3	-0.1446	-0.0730
N1-C6	1.3323	1.3512	N1-C2-C3	122.7560	123.1958	C6-N1-C2-H7	-179.0661	-178.7928
C2-C3	1.3878	1.4013	N1-C2-H7	115.9516	115.7350	C2-N1-C6-C5	0.9383	1.1008
C2-H7	1.0685	1.0812	C3-C2-H7	121.2834	121.0566	C2-N1-C6-H21	-179.5373	-179.3907
C3-C4	1.3896	1.4017	C2-C3-C4	118.0406	117.9441	N1-C2-C3-C4	-1.3254	-1.5028
C3-C8	1.4909	1.4978	C2-C3-C8	123.0641	122.9178	N1-C2-C3-C8	-175.7653	-175.0205
C4-C5	1.3841	1.3937	C4-C3-C8	118.6678	118.8276	H7-C2-C3-C4	177.5399	177.1510
C4-H19	1.0694	1.0808	C3-C4-C5	119.2523	119.2658	H7-C2-C3-C8	3.1000	3.6333
C5-C6	1.3854	1.3965	C3-C4-H19	119.4670	119.3289	C2-C3-C4-C5	2.0013	2.0596
C5-H20	1.0693	1.0811	C5-C4-H19	121.2771	121.3990	C2-C3-C4-H19	-177.3113	-177.0424
C6-H21	1.0687	1.0809	C4-C5-C6	118.5798	118.8335	C8-C3-C4-C5	176.6913	175.8494
C8-O9	1.2343	1.2593	C4-C5-H20	121.0015	120.8825	C8-C3-C4-H19	-2.6213	-3.2527
C8-N10	1.3550	1.3724	C6-C5-H20	120.4145	120.2812	C2-C3-C8-O9	135.5485	130.4607
N10-C11	1.4584	1.4681	N1-C6-C5	122.4193	122.6783	C2-C3-C8-N10	-43.3837	-48.1267
N10-C12	1.4592	1.4686	N1-C6-H21	116.2645	115.9770	C4-C3-C8-O9	-38.8584	-43.0025
C11-H13	1.0822	1.0931	C5-C6-H21	121.3145	121.3429	C4-C3-C8-N10	142.2094	138.4101
C11-	1.0750	1.0848	C3-C8-O9	118.7104	118.9827	C3-C4-C5-C6	-1.2801	-1.1290

H14								
C11-H15	1.0825	1.0932	C3-C8-N10	119.8996	119.3933	C3-C4-C5-H20	179.4521	179.4853
C12-H16	1.0744	1.0850	O9-C8-N10	121.3812	121.6084	H19-C4-C5-C6	178.0197	177.9538
C12-H17	1.0841	1.0942	C8-N10-C11	125.5922	125.4628	H19-C4-C5-H20	-1.2481	-1.4319
C12-H18	1.0807	1.0914	C8-N10-C12	118.2758	118.5603	C4-C5-C6-N1	-0.2168	-0.4968
			C11-N10-C12	115.0998	115.3582	C4-C5-C6-H21	-179.7176	-179.9795
			N10-C11-H13	115.0998	115.3582	H20-C5-C6-N1	179.0554	178.8927
			N10-C11-H14	109.0248	109.1984	H20-C5-C6-H21	-0.4453	-0.5899
			N10-C11-H15	111.5241	111.0184	C3-C8-N10-C11	-20.5379	-16.5748
			H13-C11-H14	111.2381	111.2121	C3-C8-N10-C12	171.6890	172.8871
			H13-C11-H15	107.8561	108.1876	O9-C8-N10-C11	160.5591	164.8762
			H14-C11-H15	108.2513	108.2387	O9-C8-N10-C12	-7.2141	-5.6619
			N10-C12-H16	108.8335	108.8957	C8-N10-C11-H13	-125.1856	-124.4931
			N10-C12-H17	109.9614	109.0952	C8-N10-C11-H14	-6.1960	-5.2930
			N10-C12-H18	111.2286	110.9511	C8-N10-C11-H15	115.5115	116.1244
			H16-C12-H17	108.8783	109.3882	C12-N10-C11-H13	42.9286	46.3126
			H16-C12-H18	108.4075	108.6261	C12-N10-C11-H14	161.9182	165.5127
			H17-C12-H18	109.4868	109.9665	C12-N10-C11-H15	-76.3743	-73.0699
						C8-N10-C12-H16	-27.3278	-17.7254
						C8-N10-C12-H17	92.7715	101.9092
						C8-N10-C12-H18	-147.2808	-138.0507
						C11-N10-C12-H16	163.6352	170.7957
						C11-N10-C12-H17	-76.2655	-69.5697
						C11-N10-C12-H18	43.6822	50.4704

For numbering of atoms refer Fig. 1.

Table S2 The observed (FTIR and FT-Raman) and calculated (Unscaled and Scaled) frequencies, IR intensity, Raman intensity and probable assignments (Characterized by TED) of N,N-Dimethylnicotinamide

S. No.	Observed Frequency (cm ⁻¹)		HF/6-311+G(d,p)					B3LYP/6-311+G(d,p)					Assignment (TED %)
	FTIR	FT-Raman	Calculated Frequency (cm ⁻¹)		Force constant	IR intensity	Raman intensity	Calculated Frequency (cm ⁻¹)		Force constant	IR intensity	Raman intensity	
			Unscaled	Scaled				Unscaled	Scaled				
1	-	3196	3380	3198	7.4098	14.9531	79.4177	3204	3194	6.6438	14.7215	90.0770	vCH(98)
2	-		3368	3158	7.3226	4.9025	21.3244	3189	3153	6.5527	14.2471	56.7608	vCH(98)
3	-		3365	3098	7.2948	27.6885	16.0821	3178	3091	6.5006	17.2002	12.0707	vCH(98)
4	-	3071	3350	3075	7.2080	2.1633	26.2003	3173	3069	6.4534	8.0949	42.6575	vCH(98)
5	3042	-	3306	3050	7.0685	5.3881	17.9256	3153	3045	6.4245	1.8954	16.6412	CH ₃ ss(92)
6	-	-	3297	3019	7.0200	23.2197	16.6784	3149	3015	6.3996	13.5394	18.8353	CH ₃ ss(92)
7	-	-	3220	2991	6.6960	39.3091	34.7772	3066	2984	6.0832	29.7124	48.8289	CH ₃ ips(91)
8	-	2980	3209	2968	6.6955	49.1910	43.3612	3054	2963	6.0594	39.4056	63.6513	CH ₃ ips(91)
9	2941	2940	3160	2929	6.1275	76.9283	123.3607	3006	2925	5.5429	94.7518	215.2194	CH ₃ ops(89)
10	-	2815	3152	2824	6.1075	45.7241	24.9771	3001	2818	5.5164	29.8960	17.2814	CH ₃ ops(89)
11	-	-	1781	1699	10.2984	94.5524	105.4055	1618	1693	7.7208	28.8447	129.6201	vC = O(81)
12	-	-	1759	1658	10.6324	245.6842	30.8265	1603	1654	6.9263	219.8307	95.6079	vCC(89)
13	-	-	1728	1644	8.2858	174.1734	14.6758	1581	1638	4.2912	94.2086	13.0147	vCC(88)
14	1621		1681	1629	2.1307	53.6085	36.2888	1556	1623	2.0027	37.6766	52.8239	vCC(89)
15	-	-	1661	1618	1.7349	4.4537	5.9290	1544	1612	1.4888	10.7943	10.3464	vCC(88)
16	-	1596	1657	1596	1.8281	23.6584	25.0291	1532	1592	1.5253	13.7617	29.8413	vCC(89)
17	-	-	1644	1568	1.8749	4.7231	25.5304	1524	1562	1.4589	7.1454	28.2745	vCN(90)
18	-	1516	1639	1539	2.2834	9.8117	15.9747	1512	1533	2.5475	2.1971	44.1709	vCN(90)
19	1502	-	1624	1510	2.1093	41.5465	16.2853	1495	1504	1.6824	21.9242	48.3684	v CN (89)
20	-	-	1599	1491	1.7446	6.6195	15.4054	1471	1485	1.5279	28.2979	18.6431	v CN (90)
21	1459	-	1561	1479	3.6990	293.6894	8.2152	1443	1471	2.5612	29.5262	16.6205	v CN (90)
22	-	1452	1560	1463	3.1586	26.1355	7.3746	1431	1458	3.4058	165.4976	93.1238	CH ₃ ipb(81)
23	1432	-	1487	1444	1.6482	2.0467	1.4298	1382	1440	1.4574	3.0388	1.2836	CH ₃ ipb(81)
24		-	1397	1425	4.0463	76.2407	1.0663	1278	1418	3.0775	71.8836	27.2159	CH ₃ sb(86)
25	1399	-	1357	1407	2.9091	22.7191	36.8652	1273	1400	6.9990	0.2682	5.4865	CH ₃ sb(86)
26	-	-	1334	1375	1.4747	3.8359	13.0797	1248	1368	2.4906	6.1702	37.6213	b CH(78)

27	133 2	-	1283	1344	1.3591	11.783 3	3.7025	1227	1235	1.3528	9.0403	40.2361	b CH(78)
28	-	-	1261	1292	3.8788	14.658 7	22.4574	1184	1288	1.1658	6.2682	4.0320	b CH(76)
29	127 3	-	1236	1279	1.0953	0.1956	11.1179	1142	1273	1.3408	16.336 7	11.6604	b CH(78)
30	122 1	-	1219	1238	1.7215	17.068 5	5.2914	1138	1231	0.9329	0.1193	12.9078	b CC(67)
31	120 1	-	1208	1218	1.7722	81.507 1	7.5322	1113	1213	1.4823	84.531 1	29.5831	CH ₃ opb(69)
32	119 2	1191	1181	1205	1.2278	26.938 1	15.6480	1087	1200	1.0258	12.430 2	15.9375	CH ₃ opb(69)
33	112 2	-	1141	1133	1.1117	0.4905	5.1273	1055	1130	3.0104	4.8281	236.422 4	CH ₃ opr(60)
34	109 0	-	1132	1105	2.7334	6.3731	199.297 9	1039	1097	2.0329	19.554 4	6.2460	CH ₃ opr(60)
35	106 0	-	1127	1073	2.4924	17.450 3	4.4799	1027	1068	0.8729	0.5479	0.2470	CH ₃ ipr(66)
36	104 0	1036	1112	1054	1.0792	1.7623	4.7980	995	1047	0.8527	1.9488	1.8258	CH ₃ ipr(66)
37	102 6	-	1078	1038	0.9410	1.1111	1.2057	968	1034	0.7406	2.5260	4.1857	b CN(70)
38	965	-	998	979	2.5023	2.8457	29.6997	925	973	2.1394	2.6099	35.2077	b CN(72)
39	930	-	938	942	0.9799	20.805 8	17.1500	851	936	0.8195	22.680 7	20.8996	b CN(70)
40	915	-	833	927	1.1509	62.925 9	4.8113	753	922	1.0939	14.243 6	62.2858	Rasymd(6 2)
41	-	-	811	853	2.0251	2.7835	80.0452	749	847	1.0280	35.431 6	17.1969	Rtrigd(61)
42	825	792	791	837	1.1105	18.964 0	11.0790	729	833	1.4131	5.7657	10.2962	b C = O(70)
43	745	-	713	764	1.9306	12.800 7	53.0113	660	753	1.6532	7.9858	60.8404	Rsymd(62)
44	730	-	686	750	2.0201	8.2310	31.3622	638	741	1.7487	6.6140	37.6600	g CH(62)
45	715	-	603	733	1.0216	4.2284	2.7522	560	725	0.8754	2.9698	3.4282	g CH(62)
46	-	-	490	681	0.4898	3.2660	8.0666	444	676	0.3804	1.8711	25.0956	g CH(60)
47	650	-	463	667	0.3693	3.8503	3.5218	413	659	0.2980	3.6695	3.5251	g CH(62)
48	-	625	430	642	0.4156	13.403 8	12.4260	390	633	0.3523	11.675 4	9.6194	b CC(57)
49	615	-	371	638	0.3112	1.1946	69.0672	343	626	0.2809	0.8185	71.2951	g CN(55)
50	565	-	331	584	0.2280	9.8510	35.1122	308	575	0.1837	8.4511	32.5270	g CN(54)
51	-	485	292	500	0.1904	6.9412	15.6119	272	495	0.1603	3.1739	27.3321	g CN(55)
52	-	436	234	444	0.0720	2.1926	44.4305	221	442	0.0675	1.7437	53.1193	g C = O(57)
53	-	-	173	408	0.0245	1.5729	26.1997	161	402	0.0202	1.2524	51.5648	tRtrigd(66)
54	-	-	135	364	0.0252	3.2781	438.787 3	115	457	0.0243	3.4192	672.253 4	tRsymd(6 3)
55	-	-	115	312	0.0114	1.0043	72.9727	105	315	0.0089	0.9117	142.401 8	tRasymd(60)
56	-	-	92	262	0.0153	0.6056	43.1437	87	257	0.0119	0.3721	66.8642	CH ₃ twist(58)
57	-	72	67	155	0.0119	7.6858	1290.10 15	56	151	0.0087	7.1277	2694.58 30	CH ₃ twist(56)

Abbreviations: v – stretching; b – bending; g – out-of-plane bending; t – torsion; R – ring; trigd – trigonal deformation; symd – symmetric deformation; asymd – antisymmetric deformation..